Nanomedicine: Nanotechnology, Biology, and Medicine 56 (2024) 102720

Contents lists available at ScienceDirect

Nanomedicine: Nanotechnology, Biology, and Medicine

journal homepage: www.sciencedirect.com/journal/nanomedicine-nanotechnology-biology-and-medicine

Intrinsic variability of fluorescence calibrators impacts the assignment of MESF or ERF values to nanoparticles and extracellular vesicles by flow cytometry

Estefanía Lozano-Andrés, PhD [a,*,1], Tina Van Den Broeck, PhD [b,1], Lili Wang, PhD [c], Majid Mehrpouyan, PhD [d], Ye Tian, PhD [e], Xiaomei Yan, PhD [e], Ger J.A. Arkesteijn, PhD [a,2], Marca H.M. Wauben, PhD [a,1,2]

[a] Department of Biomolecular Health Sciences, Faculty of Veterinary Medicine, Utrecht University, Utrecht, the Netherlands
[b] BD Biosciences, Erembodegem, Belgium
[c] Biosystems and Biomaterials Division, National Institutes of Standards and Technology (NIST), Gaithersburg, MD 20899, United States of America
[d] BD Biosciences, San Jose, CA 95131, United States of America
[e] Department of Chemical Biology, MOE Key Laboratory of Spectrochemical Analysis & Instrumentation, Key Laboratory for Chemical Biology of Fujian Province, College of Chemistry and Chemical Engineering, Xiamen University, Xiamen 361005, People's Republic of China

ARTICLE INFO

Keywords:
Fluorescence calibration
Standardization
Extracellular vesicles
Nanoparticles
Flow cytometry

ABSTRACT

Flow cytometry allows to characterize nanoparticles (NPs) and extracellular vesicles (EVs) but results are often expressed in arbitrary units of fluorescence. We evaluated the precision and accuracy of molecules of equivalent soluble fluorophores (MESF) beads for calibration of NPs and EVs. Firstly, two FITC-MESF bead sets, 2 and 6 um in size, were measured on three flow cytometers. We showed that arbitrary units could not be compared between instruments but after calibration, comparable FITC MESF units were achieved. However, the two calibration bead sets displayed varying slopes that were consistent across platforms.

Further investigation revealed that the intrinsic uncertainty related to the MESF beads impacts the robust assignment of values to NPs and EVs based on extrapolation into the dim fluorescence range. Similar variations were found with PE MESF calibration.

Therefore, the same calibration materials and numbers of calibration points should be used for reliable comparison of submicron sized particles.

Background

A well-known fluorescence calibration method in flow cytometry (FC) is the use of fluorescent beads to which a measurement value is assigned using standardized units established by the National Institute of Standards and Technology (NIST), such as molecules of equivalent soluble fluorophores (MESF) or equivalent number of reference fluorophore (ERF). This calibration method was developed for cellular FC and allows for quantifiable fluorescence measurements and platform comparison. Importantly, the fluorescence intensity of the calibrator beads matches the expected intensity on the labeled cells. Therefore, the calibrated cellular fluorescence variation closely compares to the intrinsic variation on the calibrator and allows for data interpolation.[1–4] In 2012, a NIST/ISAC standardization study reported differences in the assigned units to calibrators from different manufactures, indicating the importance of the examination of the accuracy and precision of available calibrators.[5] Nevertheless, the assignment of a specific MESF or ERF value to calibration beads is inextricably bound to a variation around this value. This variation translates in an uncertainty level between the measured and the assigned values that remains acceptable as long as the sample values are within the range of the calibrator.

During the last decade, small particle FC has become a powerful tool

* Corresponding author at: Department of Biomolecular Health Sciences, Faculty of Veterinary Sciences, Utrecht University, Yalelaan 1, 3584 CL Utrecht, the Netherlands.
E-mail address: e.lozanoandres@uu.nl (E. Lozano-Andrés).
[1] TRAIN-EV Marie Skłodowska-Curie Action-Innovative Training Network, train-ev.eu.
[2] Both authors contributed equally.

https://doi.org/10.1016/j.nano.2023.102720
Received in revised form 24 October 2023;
Available online 23 November 2023

for high-throughput analysis of nanoparticles (NPs) and cell-derived extracellular vesicles (EVs).[6,7] However, EV measurements are challenging, mainly because the vast majority of EVs is small in size (<200 nm) and their light scattering and fluorescent signals are typically close to, at, or below the instrument's detection limit.[8] Furthermore, the majority of data is reported in arbitrary units of fluorescence, which is cumbersome for the analysis of dim and small particles, whereby particles cannot be fully discriminated from negative counterparts and background signals. The recently published MIFlowCyt-EV framework recommends the use of MESF beads for calibration and standardized reporting of EV flow cytometric experiments, especially when a fluorescent threshold is applied.[8] However, since available calibrators are developed for cells and as such are much brighter in fluorescence than EVs it is unknown to which extend these calibrators will provide precision and/or accuracy for the assignment of fluorescent values to NPs and EVs. We investigated how the given units of the calibrator impact the regression line for assignment of MESF and/or ERF units to NPs and EVs. To this end, we evaluated custom-made calibrator beads sets from the same manufacturer on three different flow cytometers and provide insights on how different bead sets affect the calibration of fluorescence signals from NPs and EVs.

Methods

Calibration beads

For calibration of the fluorescence axis in the fluorescein isothiocyanate (FITC) channel we used two sets of FITC MESF beads: 1) Custom-made, 6 μm lot MM2307 #131-10; #131-8; #130-6; #130-5; #130-3 and 2) Custom made 2 μm lot MM2307#156; #159.1; #159.2; #122.3. For calibration of the fluorescence axis in the PE channel, we used two sets of PE MESF beads: 1) Commercial 6 μm QuantiBrite, Catalog No. 340495 lot 62981 and 2) Custom made 2 μm, lot MM2327#153.1; #153.2; #153.4; #153.5; #153.6. All four calibration bead sets were obtained from BD Biosciences, San Jose, CA.

The 6 μm FITC MESF beads were prepared by reacting various concentration of FITC with PMMA Beads (Bangs Labs) in borate buffer at pH 9.2. The 2 μm FITC beads were prepared by reacting various concentrations of FITC-BSA (with a FITC/BSA molar ratio of 2) with 2 μm carboxylic beads (Bangs Labs) using EDC/NHS chemistry. The 2 μm PE beads were made as described above except various concentrations of PE were used with 2 μm carboxylic beads in EDC/NHS chemistry. These beads were analyzed on a BD LSRFortessa™ (BD Biosciences) and their MESF values were assigned by cross-calibration using commercially available MESF beads (Flow Cytometry Standards Corp.). The FITC ERF values were assigned to both 2 μm and 6 μm beads using a specific lot of FITC-FC Bead (BD Biosciences) as a calibrator with known ERF value, which has been assigned by NIST. This provided us with two distinct calibrator bead sets that were produced through the same manufacturing process and assigned using the same instruments and the same internal NIST traceable calibrator to exclude internal processing variations.

In addition, we measured commercially available Quantum™ FITC-5 MESF (7 μm, Catalog No. 555, lot 14609, Bangs Laboratories) and AccuCheck ERF Reference Particles Kit (3 μm, Catalog No. A55950, lot #081220207, #081220203, #081220208, Thermo Fisher) which were prepared according to the manufacturer's instructions.

All calibration bead sets were measured with gain or voltage settings as would be used for the analysis of small particles (i.e., EVs). In addition, not all beads could be measured on every instrument. For fair cross-platform comparison of the slopes of the regression lines, only the bead populations that could be measured on all instruments were included for linear regression analysis.

Flow cytometer platforms

In this study three flow cytometers were used. A jet in air-based BD Influx (BD Biosciences, San Jose, CA), a BC CytoFLEX LX (Beckman Coulter, Brea, CA) with a cuvette-based system and a cuvette-based SORP BD FACSCelesta™ (BD Biosciences, San Jose, CA) equipped with a prototype small particle side scatter module.

The BD Influx flow cytometer was modified and optimized for detection of submicron-sized particles.[9] In brief, FITC was excited with a 488 nm laser (Sapphire, Coherent 200 mW) and fluorescence was collected through a 530/40 bandpass filter. PE was excited with a 562 nm laser (Jive, Cobolt 150 mW) and fluorescence was collected through a 585/42 bandpass filter. Optical configuration of the forward scatter detector was adapted by mounting a smaller pinhole and an enlarged obscuration bar in order to reduce optical background. This reduced wide-angle FSC (rwFSC) allowed detection of sub-micron particles above the background based on forward scatter.[9,10] Upon acquisition, all scatter and fluorescence parameters were set to a logarithmic scale. To minimize day to day variations, the BD Influx was standardized at the beginning of each experiment by running 100 and 200 nm yellow-green (505/515) FluoSphere beads (Invitrogen, F8803 and F8848). The instrument was aligned until predefined MFI and scatter intensities where reached with the smallest possible coefficient of variation (CV) for rwFSC, SSC and fluorescence. After optimal alignment, PMT settings required no or minimal day to day adjustment and ensured that each measurement was comparable. MESF beads and NPs were measured with a FSC threshold set at 1.0 while for biological EVs a fluorescence threshold was set at 0.67 by allowing an event rate of 10–20 events/s while running a clean PBS control sample.

When performing quantitative and qualitative analysis of synthetic NPs and biological EVs, preparations were diluted in PBS as indicated. Upon loading on the Influx, the sample was boosted into the flow cytometer until events appeared, after which the system was allowed to stabilize for 30 s. Measurements were performed either by a fixed 30 s time or by setting a gate around the spike-in beads and allowing to record a defined number of events in the gate (80,000 events) using BD FACS Sortware 1.01.654 (BD Biosciences).

The CytoFLEX LX was used without any tailor-made modifications in the configuration. Before measurements, the manufacturer recommended startup and QC procedure were run first. All scatter and fluorescence parameters were set to a logarithmic scale. FITC was measured with a 50 mW 488 nm laser and fluorescence was measured through a 525/40 band pass filter at gain 1.0. FITC MESF beads were recorded with an FSC threshold at 1000. Measurements were performed using CytExpert 2.1 (Beckman Coulter).

The SORP BD FACSCelesta™ was equipped with a prototype small particle SSC module for improved scatter detection. Before measurement, the recommended CS&T performance check was run to monitor performance on a daily basis and to optimize laser delay. All scatter and fluorescence parameters were set to a logarithmic scale. 100 nm yellow-green (505/515) FluoSphere beads (Invitrogen, F8803) were acquired and used to set optimal fluorescence (FITC detector) PMT-V values. FITC was measured with a 100 mW 488 nm laser through a 530/30 band pass filter. FITC-MESF beads were recorded with an SSC threshold at 200. Measurements were performed using BD FACSDiva™ Software v8.0.3 (BD Biosciences).

Further descriptions of each instrument and methods are provided in Data S1 (MIFlowCyt checklist) and Data S2 (MiFlowCyt-EV framework).

Preparation of FITC-doped silica nanoparticles

Synthetic silica nanoparticles (SiNPs) of 550 nm diameter with six different FITC fluorescence intensities were produced by using a modified method of literature reports.[11–13] Briefly, the amine reactive FITC molecules were covalently linked to the silane coupling agent, (3-aminopropyl)-triethoxylsilane (APTES) in anhydrous ethanol.

Monodisperse silica seeds of ~90 nm prepared by using amino acid as the base catalyst[11,12] were suspended in a solvent mixture containing ethanol, water and ammonia. Then tetraethyl orthosilicate (TEOS) and different volumes of APTES−FITC solutions were added for growing FITC-doped SiNPs by a modified Stöber method.[13,14] Upon washing three times with anhydrous ethanol, the FITC-doped SiNPs were reacted with TEOS in the solvent mixture to allow growth of a silica layer. The synthesized SiNPs were washed three times with anhydrous ethanol and stocked in anhydrous ethanol. The diameters of SiNPs were measured by transmission electron microscopy.

Isolation and fluorescent staining of extracellular vesicles for flow cytometric analysis

EV-containing samples were obtained from 4T1 mouse mammary carcinoma cell culture supernatants (ATCC, Manassas, VA) as previously described.[10,15,16] EVs were stained with 5-(and-6)-Carboxyfluorescein diacetate succinimidyl ester (CFDA-SE, hereinafter referred as CFSE) (Thermo Fisher, Catalog No. C1157) and separated as described previously.[9] Briefly, 2 μl of the isolated 4T1 EVs (corresponding to a concentration of 1.44 E12 particles/ml as determined by nanoparticle tracking analysis) were mixed with 18 μl PBS/0.1 % aggregate-depleted (ad)BSA. For antibody labeling, samples were first resuspended in 15.5 μl PBS/0.1 % adBSA and incubated with 0.5 μg of rat anti-mouse CD9-PE (Clone: KMC8, IgG2a, κ, lot 7268877, BD Biosciences) or matched isotype antibodies (Rat IgG2a, κ, PE-conjugated, lot 8096525, BD Biosciences) for 1 h at RT while protected from light. EVs were then stained with 40 μM CFSE in a final volume of 40 μl. The sealed tube was incubated for 2 h at 37 °C while protected from light. Next, staining was stopped by adding 260 μl PBS/0.1 % adBSA. After fluorescent staining, EVs were separated from protein aggregates and free reagents by bottom-up density gradient centrifugation in sucrose for 17.30 h at 192,000*g* and 4 °C using a SW40 rotor (k-factor 144.5; Beckman Coulter, Fullerton, California, USA). Twelve fractions of 1 ml were then collected from the top of the gradient and respective densities were determined by refractometry using an Atago Illuminator (Japan). For analysis by flow cytometry, EV samples corresponding to a 1.14 g/ml density were diluted 1:20 in PBS prior measurement. MIFlowCyt-EV framework[8] were followed whenever applicable (Data S2).

Concentration determination by using spike-in beads

EV concentration was normalized using a spiked-in external standard containing 200 nm orange (540/560) fluorescent beads (Invitrogen, F8809). The concentration of the beads was determined by Flow NanoAnalyzer N30 (NanoFCM, Xiamen, China) and stocked at 5.7E10 particles/ml. Beads were diluted $1{:}10^4$ in PBS and added to the EV samples, mixed and measured on the flow cytometer. Bead count was used to calculate the EV concentration for BD Influx measurements.

Data analysis

For fluorescence calibration each bead peak population was gated using FlowJo Version 10.5.0 and MFI were obtained for further least square linear regression analysis. Data was handled in Microsoft Excel and figures were prepared using GraphPad Prism version 8.0 (GraphPad Software Inc). The software FCMPASS Version v2.17 was used to generate files with calibrated axis units in the histograms and dot plots shown[17] (Software is available on http://go.cancer.gov/a/y4ZeFtA).

Results

Assessment of precision and accuracy of different MESF bead sets for fluorescence calibration across platforms

To assess the precision and accuracy of MESF bead sets for fluorescence calibration across platforms, two FITC MESF bead sets of 6 μm and 2 μm, containing respectively five or four fluorescent bead populations, were selected for measurements on three different instruments, namely a BD Influx, a BC CytoFLEX and a SORP BD FACSCelesta™. Since calibrator bead sets can differ in the number of fluorescent bead populations (typically ranging from 3 to 5) and the number of calibrator points can impact the slope of the regression line (Fig. S1a–b), we included for fluorescence calibration across platforms equal numbers of fluorescent bead populations (n = 4) of the two FITC MESF bead sets that were consistently measured on all three platforms (Fig. 1).

Singlet gated populations are displayed as overlays in histograms showing the FITC fluorescence (Fig. 1a) and indicated from dim to bright as p1, p2, p3 and p4 (Fig. 1b). The 6 μm FITC MESF beads contained overall brighter fluorescent intensities, whose assigned values range from 25,910 to 715,225 FITC MESF, while the 2 μm FITC MESF beads covered a dimmer part of the fluorescence intensity range with assigned values ranging from 3634 to 103,706 FITC MESF. Clearly, MFI arbitrary units cannot be directly compared between instruments (Fig. 1b), but after fluorescence calibration comparable FITC MESF units could be assigned (Fig. 1c–d). Nevertheless, the two calibration bead sets displayed a different slope with a consistent tendency across the three platforms, suggesting a variation introduced by an inherent attribute of the beads themselves. This led us to further examine the robustness of the calibration. To gain insight into the precision and accuracy of MESF assignments we selected specific bead populations from one set, referred to as 'unknown' in Fig. 1d, to recalculate their FITC MESF units using the regression line from the other bead set. The selected 'unknown' samples used were: (i) p1 and p4 of the 2 μm bead set for which the FITC MESF values were calculated using the regression line of the 6 μm bead set and (ii) p1 and p2 of the 6 μm bead set for which the FITC MESF values were calculated using the regression line of the 2 μm bead set (Fig. 1c). Using this approach, the calculated MESF values of p4 from the 2 μm beads and p2 from the 6 μm beads showed <20 % variation (10 % above or 10 % below actual values) of the actual value, while data were precise when compared between platforms (Fig. 1d). Also the MESF values of the dimmest p1 2 μm and 6 μm beads, calculated using respectively the regression lines of the 6 μm and 2 μm bead sets, were comparable between platforms. However, the calculated values revealed more than a 20 % variation from the given value, leading to either an underestimation or an overestimation of the FITC MESF units (Fig. 1d). These results show that slight differences in the slope of the calibration lines of the different MESF bead sets become more prominent when extrapolation needs to be extended into the dim area beyond the fluorescence intensities of the calibration beads themselves. Since the same slope differences occurred on all three platforms (Fig. 1c), this observation is not related to the type of instrument used (e.g.; digital or analog, photomultiplier (PMT) or avalanche photodiode (APD), jet-in-air or cuvette based). Furthermore, this recurring pattern on all platforms makes it unlikely that differences in slopes were caused by instrument non-linearity. Further evidence to rule out non-linearity issues is provided by linear plotting of the values, showing no non-linearity issues (Fig. S2a–c), and demonstrating instrument linearity on the BD Influx following the approach described by Bagwell et al.[19] (Fig. S3). Furthermore, we ruled out that slope differences were a result of variations between separate measurements (Fig. S4) and confirmed by testing both custom-made and commercial FITC MESF beads (Fig. S1) and FITC MESF beads and PE MESF beads (Fig. S2d–f) that slope variability is inherent to the use of calibrator beads.

MESF assignments of FITC fluorescence intensities to synthetic silica nanoparticles depend on the MESF-bead calibrator set

We next investigated how calibration with the two FITC MESF bead sets of 6 μm and 2 μm impacts fluorescent assignment to dim fluorescent nanoparticles. For this purpose, 550 nm silica NPs containing 6

a

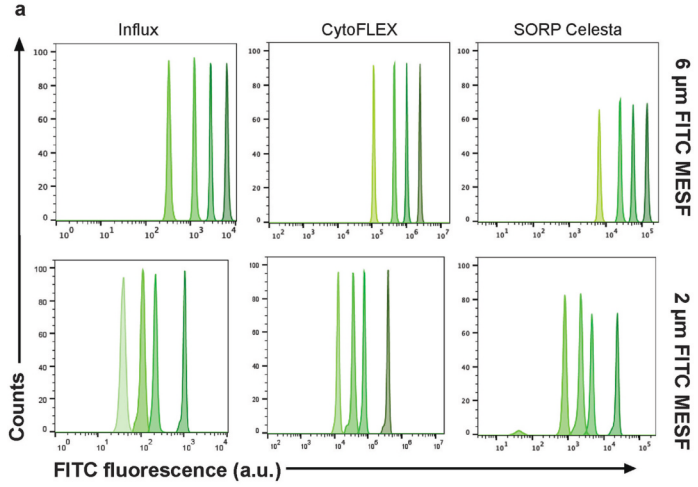

b

Brightness	6 µm beads	MFI Influx	MFI CytoFLEX	MFI SORP Celesta	FITC MESF
	p1	317	107336	6321	25910
	p2	1173	421852	23322	118192
	p3	2684	962928	53219	275288
	p4	6111	2324148	127668	715225

Brightness	2 µm beads	MFI Influx	MFI CytoFLEX	MFI SORP Celesta	FITC MESF
	p1	37	12357	780	3634
	p2	106	34544	2169	10520
	p3	210	73054	4380	22841
	p4	991	367458	22370	103706

c

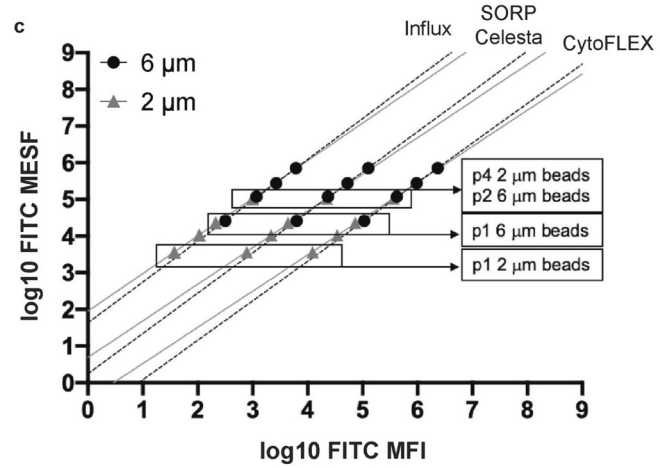

	6 µm FITC MESF beads	2 µm FITC MESF beads
Influx	Y = 1.1146*X + 1.6325 R^2 = 0.9995	Y = 1.0261*X + 1.951 R^2 = 0.9993
CytoFLEX	Y = 1.0762*X – 0.9947 R^2 = 0.9998	Y = 0.9869*X – 0.4632 R^2 = 0.9992
SORP Celesta	Y = 1.1004*X – 0.2432 R^2 = 0.9993	Y = 0.9989*X + 0.6884 R^2 = 0.9985

d

Used as calibrator	Used as unknown	Assigned FITC MESF Given values	Calculated FITC MESF values Influx	CytoFLEX	SORP Celesta
6 µm FITC beads	p4:::2 µm FITC beads	103706	93745	98759	107046
2 µm FITC beads	p2:::6 µm FITC beads	118192	125680	122538	112554
6 µm FITC beads	p1:::2 µm FITC beads	3634	2432	2565	2665
2 µm FITC beads	p1:::6 µm FITC beads	25910	32904	31743	30550

Fig. 1. Evaluation of two different FITC MESF bead sets for the calibration of fluorescent intensities across three flow cytometer platforms. **(a)** Histogram overlays (axis in arbitrary units) of FITC fluorescent intensity peaks derived from the 6 µm (upper row) or the 2 µm (lower row) FITC MESF beads. **(b)** Table showing the median fluorescence intensity (MFI) statistic derived from each of the fluorescent intensity peaks from dimmer to brighter being expressed in arbitrary units as well as the assigned MESF values (right column). **(c)** Least square linear regression analysis of 6 µm (black circles) and 2 µm (grey triangles) FITC MESF beads. Provided FITC MESF and measured FITC MFI values were transformed to log and plotted in a log-log fashion for the three platforms. **(d)** Table indicating the expected and calculated FITC MESF values for each sample used in the analysis. The experiment shown is representative for two independently performed experiments on the Influx and CytoFLEX, measurements on the SORP Celesta were done once.

populations with FITC fluorescence intensities below or within the range of the calibration beads were measured on the BD Influx. Singlets were gated (Fig. S5) and histogram overlays were generated showing 6 different FITC fluorescence intensities (Fig. 2a, left). Histograms showing the calibrated FITC MESF units of these silica NPs based on fluorescence calibration with either the 6 µm or 2 µm FITC MESF calibrator bead set are displayed in Fig. 2a (respectively middle or right). The obtained MFI and CV values for each silica NP population, as well as the calculated FITC MESF values based on the two calibrator sets are shown in Fig. 2b. The calculated FITC MESF values for the silica NPs appeared consistently lower when the regression line of the 6 µm calibration bead sets was used (Fig. 2b). This phenomenon is not limited to the use of FITC MESF beads and can solely be explained by the difference in the slope of the regression line of the two calibrator bead sets, as was confirmed by calculating the fluorescent intensity in terms of PE ERF for 200 nm broad spectrum fluorescent polystyrene NPs based on the 6 µm and 2 µm PE MESF calibrator bead sets (Fig. S6a). Importantly, multi-intensity peak analysis of the silica NPs revealed that the difference in FITC MESF values of these NPs obtained by the two calibrator bead sets increased in the dimmer range of the fluorescence, with 27.3 % variation for the brightest fluorescent peak (p6) to 76.5 % variation for the dimmest population of these NPs (Fig. 2b). Also the PE ERF values calculated for the relatively dim 200 nm broad spectrum fluorescent polystyrene NPs based on the 6 µm or 2 µm PE MESF calibrator bead sets showed a variation of 41.3 % (Fig. S6a). These results can be explained by the fact that the differences in calculated values increase by extrapolation into the dim area as a consequence of the differences in the slopes of the regression lines between the calibrator bead sets.

a

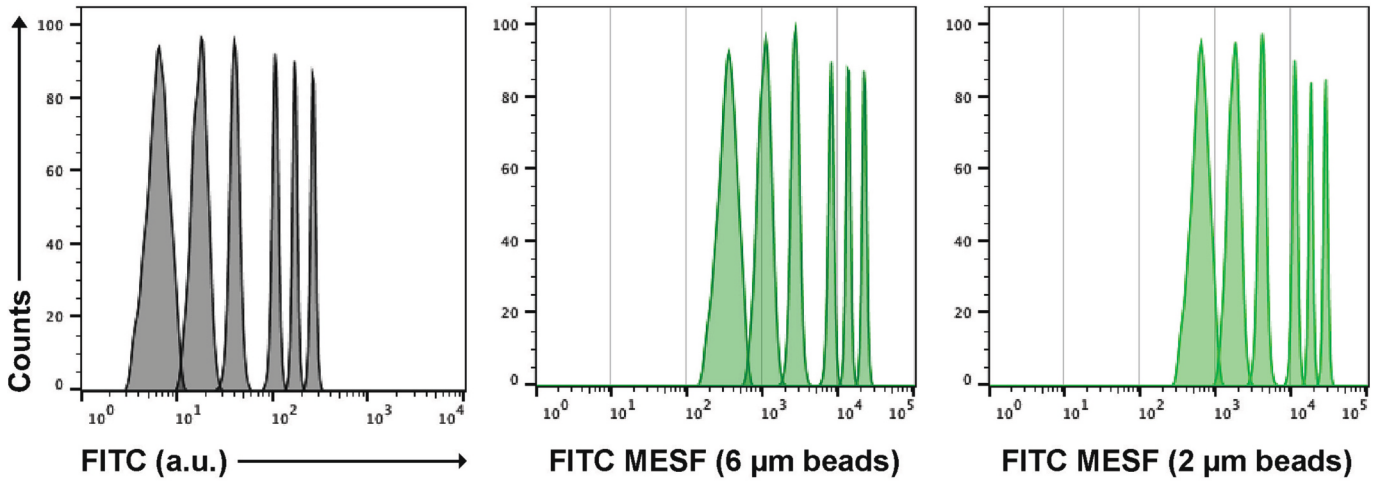

b

			Calculated FITC MESF values Used as calibrator		
Unknown	MFI	CV	6 µm FITC beads	2 µm FITC beads	% variation
p1	6.35	25.53	337	595	76.5
p2	17.20	17.83	1022	1654	61.8
p3	39.60	10.89	2590	3894	50.3
p4	104.90	6.86	7671	10581	37.9
p5	167.00	5.12	12881	17050	32.4
p6	258.90	5.10	20995	26734	27.3

Fig. 2. MESF bead-based calibration of fluorescence signals from synthetic silica NPs. **(a)** Histogram overlay showing FITC fluorescence in arbitrary units (a.u.) (left), FITC MESF calibrated axis based on the 6 µm (middle) and 2 µm FITC MESF beads (right) from the six differently FITC-labeled 550 nm NP gated populations. **(b)** Table showing the MFI and CV as well as the calculated FITC MESF values for each of the unknown populations with the percentage of variation between the two calculated reference values.

MESF calibration using different bead sets leads to variable ERF and MESF values assigned to fluorescently CFSE stained and CD9 labeled extracellular vesicles

We next demonstrate the impact of the assignment of FITC ERF units and PE MESF units to a biological EV sample measured on the BD Influx by using the four different MESF calibrator sets, i.e., 6 and 2 µm FITC MESF and 6 and 2 µm PE MESF beads. Since the light scatter of these EVs was too low to resolve the EV population from the background signals, fluorescence thresholding was applied[9] based on CFSE staining. Furthermore, the expression of CD9, a tetraspanin enriched on the surface of the 4 T1-derived EVs, was analyzed by using a CD9-PE antibody (Fig. 3a). Unstained EVs and CFSE stained EVs with a matching isotype-PE control were measured side-by-side (Fig. 3a) and fluorescent polystyrene spike-in beads (200 nm) were added to EV samples to determine the EV-concentration and define the EV-gating (Fig. S7a). In Fig. 3c–d, the histogram overlays show how the fluorescence intensities of the calibrators relate to the fluorescent signals generated by CFSE stained and CD9-PE labeled EVs. Fluorescent calibration revealed a 76.6 % variation in the calculated CFSE ERF units of CFSE stained EV and a 156.9 % variation in the calculated PE MESF units of CD9-PE labeled EVs when the different MESF calibrator sets were used (Fig. 3a–b). Moreover, the fluorescent threshold value of 0.67 used on the BD Influx corresponds to an equivalent of 150 FITC MESF based on the 6 µm beads or 300 FITC MESF based on the 2 µm beads (Fig. 3a), which also shows the variation between two bead sets when reporting the level of detection in standardized units.

Discussion

The field of small particle flow cytometry is rapidly evolving, where the definition of what and how much can be detected is crucial. Besides the inter-comparability of data, the use of MESF/ERF values generates awareness about the range of fluorescence intensities that can be expected for small particles, such as EVs, and allows to indicate instrument detection sensitivity and to report fluorescence thresholding in calibrated units.[8,20]

In line with previous findings, we here showed that linear regression curves derived from four calibration bead sets we tested, which were developed for calibration of fluorescence on cells, can be used to calculate MESF/ERF values for dim NPs and EVs and allows for data inter-comparability with acceptable precision when the same calibrator set is used in the three instruments that we have tested.[20] Since earlier reports pointed out towards variabilities in MESF/ERF assignments

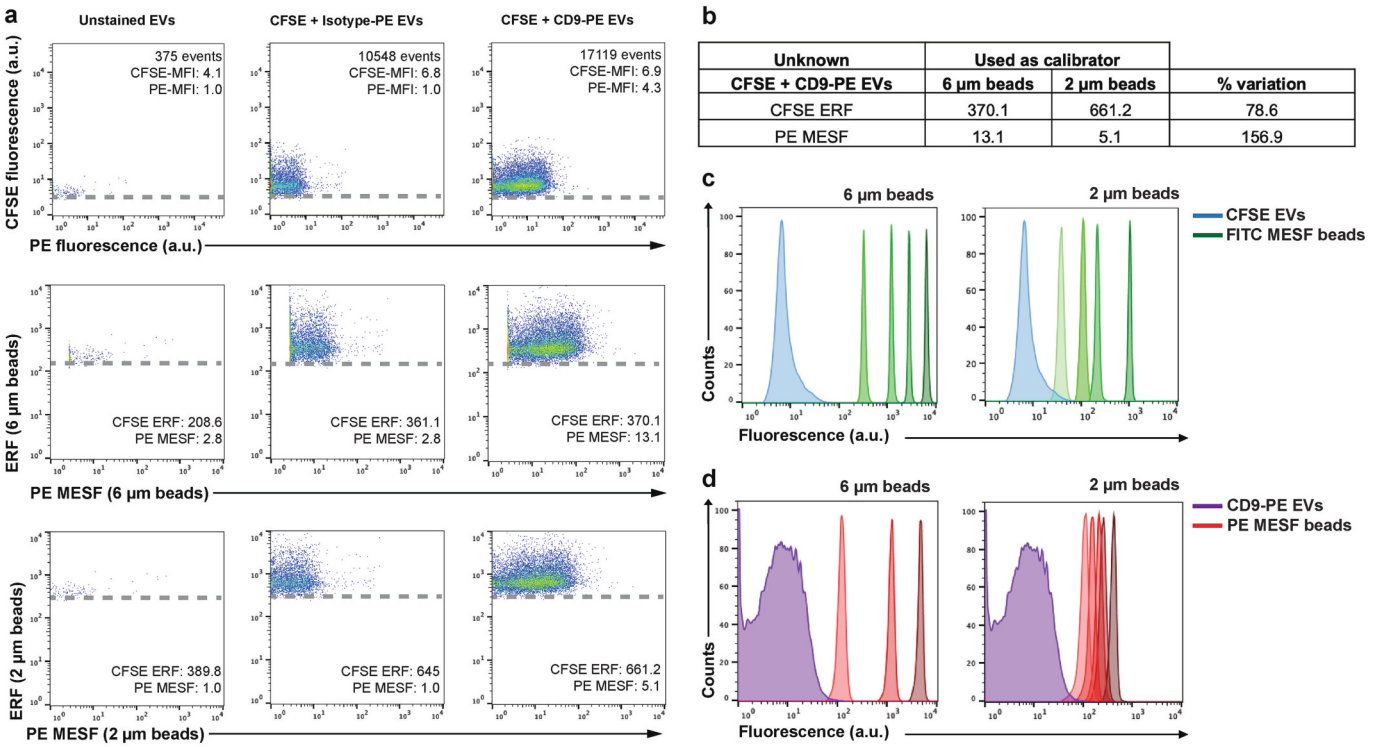

Unknown	Used as calibrator		
CFSE + CD9-PE EVs	6 µm beads	2 µm beads	% variation
CFSE ERF	370.1	661.2	78.6
PE MESF	13.1	5.1	156.9

Fig. 3. MESF bead-based calibration of fluorescent signals from biological EV samples. **(a)** Analysis of EV samples by using a fluorescence threshold. Unstained EVs control (left), CFSE and isotype-PE stained EVs (middle) and CFSE and CD9-PE stained EVs (right) dot plots showing CFSE fluorescence Vs PE fluorescence in arbitrary units (a.u.) (upper row) or CFSE ERF Vs PE MESF calibrated axis based on either the 6 µm (middle row) or 2 µm calibration beads (lower row). The dashed line in each dot plot indicates the fluorescence threshold value used. Number of events within the EV gate and MFI values for either CFSE or PE fluorescence (a.u.) are indicated in the top row. CFSE ERF and PE MESF values are indicated based on the 6 µm (middle row) or 2 µm beads (lower row). **(b)** Table showing the ERF or MESF values obtained after calibration for the CFSE and CD9-PE stained EVs and the percentage of variation between the use of the 6 µm or 2 µm bead sets. **(c)** Histogram overlays displaying fluorescence in arbitrary units from CFSE stained EVs (blue) next to the 6 µm or 2 µm FITC-MESF bead set (green). **(d)** Histogram overlays displaying fluorescence in arbitrary units from CD9-PE labeled EVs (purple) next to the 6 µm or 2 µm PE-MESF bead set (red). (For interpretation of the references to color in this figure legend, the reader is referred to the web version of this article.)

between manufacturer's,[5] we used different calibrator bead sets from the same manufacturer, assigned by using the same method and internal NIST traceable calibrator and prepared by following the same manufacturing process. Nevertheless, we found that the robustness of a calculated MESF/ERF value varies upon the use of different calibrator bead sets.

We here demonstrate that the calibration of dim NPs and EVs is substantially affected by the intrinsic variation within the assignment of MESF/ERF values to the calibrator beads.[21] In metrology it is known that every measurement has an intrinsic uncertainty around the given value and the acceptable range of variation is strictly defined for each standard. However, the uncertainties in MESF/ERF assignment to calibrator beads are not always provided by manufacturers. Since the fluorescent intensities of EVs, based on generic staining and/or on antibody labeling, are far dimmer than the available calibrators, calculation of their MESF/ERF values relies on extrapolation of the regression line of the calibrator beads into the dim area. When using different calibrator sets, their variations in the intrinsic uncertainties of the assigned values will be enlarged during extrapolation. Indeed, our data clearly demonstrate that regression lines of different calibrator sets resulted in different calculated MESF/ERF values for NPs and EVs that have fluorescent intensities at the lower end or below the intensities of the calibrator beads themselves. This was caused by the increased separation of regression lines with slightly different slopes at the lower end and increased the uncertainties in the MESF/ERF assignment for dim NPs and EVs, thereby compromising the accuracy of the MESF/ERF assignment.

Importantly, most commercially available calibrator bead sets do not provide uncertainty values around the given MESF/ERF units, which would help to create awareness about the possibilities and limitations related to MESF/ERF unit reporting. The reporting of such uncertainty values might also help to improve the accuracy by combining multiple calibrators and reference materials. For such approach, inter-laboratory studies testing more commercially available bead sets with reported uncertainty values from distinct vendors, analyzed on a wide array of different flow cytometers including the newer generation platforms with higher sensitivity for the detection of small particles, will be helpful.

However, based on our current findings, the use of the same calibrator bead set and the same number of data points of the calibrators used for linear regression is recommended to increase robustness of the calculation of MESF/ERF values for inter-laboratory and inter-platform comparison, and detailed description of calibration materials and calculation of MESF/ERF values would increase reproducibility.

Clearly, a calibrator with MESF/ERF values closer to the range of fluorescence intensities of the sample of interest and with a low uncertainty of assignment is preferable. Moreover, novel state-of-the-art flow cytometers that are designed to measure small particles rely obligately on sub-micron sized beads to perform MESF/ERF calibration. These state-of-the-art platforms cannot measure the 'standard' 6 µm MESF beads.[22] Therefore, there is an urgent need for the development of a new generation traceable calibration beads to advance the characterization of synthetic and biological particles in the nanometric scale range.

In summary, our results illustrate how fluorescence calibration can enable data comparison and provide information on the detection sensitivity of the instrument in standardized units,[23,24] but also urge for awareness of the limitations when fluorescence calibration is being

employed for EVs and NPs, especially in terms of accuracy. Lastly, for robust assignments of fluorescence values to NPs and EVs, there is a need for multi-institutional collaborations (between research labs, companies and metrology institutions, such as NIST) to produce and validate calibration materials that have low and well-characterized uncertainty of assigned fluorescent values, ideally allowing for data interpolation and with a size range that is compatible for all flow cytometer platforms.

Funding statement

This research is supported by the European Union's Horizon 2020 research and innovation programme under the Marie Skłodowska-Curie (grant agreement No 722148) and by the National Natural Science Foundation of China (21934004 and 21627811). E. L. A. is supported by the European Union's Horizon 2020 research and innovation programme under the Marie Skłodowska-Curie grant agreement No 722148.

CRediT authorship contribution statement

Estefanía Lozano-Andrés: Conceptualization, Data curation, Formal analysis, Investigation, Methodology, Resources, Software, Writing – original draft. **Tina Van Den Broeck:** Conceptualization, Investigation, Methodology, Resources, Writing – review & editing. **Lili Wang:** Methodology, Writing – review & editing. **Majid Mehrpouyan:** Conceptualization, Investigation, Methodology, Resources, Writing – review & editing. **Ye Tian:** Investigation, Methodology, Resources, Writing – review & editing. **Xiaomei Yan:** Conceptualization, Investigation, Methodology, Resources, Writing – review & editing. **Ger J.A. Arkesteijn:** Conceptualization, Data curation, Formal analysis, Investigation, Methodology, Resources, Supervision, Validation, Software, Writing – original draft. **Marca H.M. Wauben:** Conceptualization, Data curation, Formal analysis, Funding acquisition, Investigation, Methodology, Project administration, Resources, Supervision, Validation, Writing – original draft.

Declaration of competing interest

Tina Van Den Broeck and Majid Mehrpouyan are both employees of BD Biosciences, a business unit of Becton, Dickinson and Company. During the course of this study, the Wauben research group, Utrecht University, Faculty of Veterinary Medicine, Department of Biomolecular Health Sciences and BD Biosciences collaborated as a co-joined partner in the European Union's Horizon 2020 research and innovation programme under the Marie Skłodowska-Curie grant agreement No 722148. Xiaomei Yan declares competing financial interests as a cofounder of NanoFCM Inc., a company committed to commercializing the nano-flow cytometry (nFCM) technology.

Data availability

All EV data of our experiments have been submitted to the EV-TRACK knowledgebase (EV-TRACK ID: EV210047).[18] All flow cytometric data files have been deposited at the Flow Repository (FR-FCM-Z3FJ).

Acknowledgments

The authors would like to thank Prof. An Hendrix (Laboratory of Experimental Cancer Research, Ghent University, Belgium) for the possibility to prepare and analyze M4T1 derived EV in her lab and Ludo Monheim (BD Biosciences, Erembodegem, Belgium) for helpful technical support.

Appendix A. Supplementary data

Supplementary data to this article can be found online at https://doi.org/10.1016/j.nano.2023.102720.

References

1.. Hoffman RA. Standardization, calibration, and control in flow cytometry. *Curr Protoc Cytom*. 2005:3 [**Chapter 1**: p. Unit 1].
2.. Wang L, Hoffman RA. Standardization, calibration, and control in flow cytometry. *Curr Protoc Cytom*. 2017;79 [p. 1 3 1-1 3 27].
3. Gaigalas AK, et al. Quantitating fluorescence intensity from fluorophore: assignment of MESF values. *J Res Natl Inst Stand Technol*. 2005;110(2):101–114.
4. Wang L, et al. Quantitating fluorescence intensity from fluorophores: practical use of MESF values. *J Res Natl Inst Stand Technol*. 2002;107(4):339–353.
5. Hoffman RA, et al. NIST/ISAC standardization study: variability in assignment of intensity values to fluorescence standard beads and in cross calibration of standard beads to hard dyed beads. *Cytometry A*. 2012;81(9):785–796.
6. Nolan JP. Flow cytometry of extracellular vesicles: potential, pitfalls, and prospects. *Curr Protoc Cytom*. 2015;73 [p. 13 14 1-16].
7. Lian H, et al. Flow cytometric analysis of nanoscale biological particles and organelles. *Annu Rev Anal Chem (Palo Alto Calif)*. 2019;12(1):389–409.
8.. Welsh JA, et al. MIFlowCyt-EV: a framework for standardized reporting of extracellular vesicle flow cytometry experiments. *J Extracell Vesicles*. 2020;9(1):1713526.
9. van der Vlist EJ, et al. Fluorescent labeling of nano-sized vesicles released by cells and subsequent quantitative and qualitative analysis by high-resolution flow cytometry. *Nat Protoc*. 2012;7(7):1311–1326.
10. Arkesteijn GJA, et al. Improved flow cytometric light scatter detection of submicron-sized particles by reduction of optical background signals. *Cytometry A*. 2020;97(6):610–619.
11. Yokoi T, et al. Periodic arrangement of silica nanospheres assisted by amino acids. *J Am Chem Soc*. 2006;128(42):13664–13665.
12. Yokoi T, et al. Mechanism of formation of uniform-sized silica nanospheres catalyzed by basic amino acids. *Chem Mater*. 2009;21(15):3719–3729.
13. Stöber W, Fink A, Bohn E. Controlled growth of monodisperse silica spheres in the micron size range. *J Colloid Interface Sci*. 1968;26(1):62–69.
14. Giesche H. Synthesis of monodispersed silica powders II. Controlled growth reaction and continuous production process. *J Eur Ceram Soc*. 1994;14(3):205–214.
15.. Vergauwen G, et al. Confounding factors of ultrafiltration and protein analysis in extracellular vesicle research. *Sci Rep*. 2017;7(1):2704.
16.. Geeurickx E, et al. The generation and use of recombinant extracellular vesicles as biological reference material. *Nat Commun*. 2019;10(1):3288.
17. Welsh JA, Horak P, Wilkinson JS, Ford VJ, Jones JC, Smith D, Holloway JA, Englyst NA. FCM_{PASS} software aids extracellular vesicle light scatter standardization. *Cytometry A*. 2020;97(6):569–581. https://doi.org/10.1002/cyto.a.23782. Jun; Epub 2019 Jun 28. PMID: 31250561; PMCID: PMC7061335.
18.. Consortium, E.-T, et al. EV-TRACK: transparent reporting and centralizing knowledge in extracellular vesicle research. *Nat Methods*. 2017;14(3):228–232.
19. Bagwell CB, et al. A simple and rapid method for determining the linearity of a flow cytometer amplification system. *Cytometry*. 1989;10(6):689–694.
20. Welsh JA, Jones JC. Small particle fluorescence and light scatter calibration using FCMPASS software. *Curr Protoc Cytom*. 2020;94(1), e79.
21.. Draper NR, Smith H. *Applied regression analysis*. New York: Wiley; 1981.
22. Tian Y, et al. Protein profiling and sizing of extracellular vesicles from colorectal cancer patients via flow cytometry. *ACS Nano*. 2018;12(1):671–680.
23. Welsh JA, Jones JC, Tang VA. Fluorescence and light scatter calibration allow comparisons of small particle data in standard units across different flow cytometry platforms and detector settings. *Cytometry A*. 2020;97(6):592–601.
24. Nolan JP, Stoner SA. A trigger channel threshold artifact in nanoparticle analysis. *Cytometry A*. 2013;83(3):301–305.